# Supporting Information (*SI*)

**Infant Brain Responses to Felt and Observed Touch of Hands and Feet: An MEG Study**

**Meltzoff, Ramírez, Saby, Larson, Taulu, & Marshall**

***Developmental Science*** **doi: 10.1111/desc.12651**

## SI Methods

**1. ECD Modeling.** Single dipole fits were calculated from the SEFs (low-pass filtered at 40 Hz) using a spherical volume conduction model and 117 sensors (78 gradiometers and 39 magnetometers) over the somatosensory cortex. Based on the grand average waveforms, for the early responses, dipoles were fitted every 1 ms from 70 to 100 ms for the hand condition and from 70 to 125 ms for the foot condition. For the late responses, dipoles were fitted every 1 ms from 175 to 325 ms for both conditions. The average GOF for the selected ECDs was 88.7% (range 60.8%–98.2%; *SD* = 8.3). For each subject and condition, the dipole with the best GOF within the defined time window was selected for further group analysis. We tested whether the dipole coordinates were significantly different for the hand condition compared to the foot condition (see main paper and Table 1).

**2. eLORETA.**

***2.1. Anatomical and Forward Modeling.*** A template source space made of cortical surfaces (~20,000 source points) and sub-cortical volumes (~6000 voxels) was constructed from the segmentation of an MRI of one 14-month-old subject. The template scalp surface was aligned and warped to optimally fit each subject's digitized head points, and the resulting transformation was applied to the template source space and the inner skull surface. Forward modeling was done using the Boundary Element Method (BEM) with the isolated skull approach (Hämäläinen & Sarvas, 1989).

***2.2. eLORETA Source Imaging.*** Source analysis was done with the eLORETA inverse algorithm (Pascual-Marqui, 2007; Pascual-Marqui et al., 2011) without dipole orientation constraints using gradiometers and magnetometers. The eLORETA current density estimates are weighted minimum-L2-norm solutions (i.e., Bayesian maximum a posteriori estimates with Gaussian prior), in which the a priori source covariance matrix is optimized to achieve zero localization bias (i.e., the maximum of each estimated point-spread function is located at the true location of each modeled dipole). The noise covariance was computed from the pre-stimulus time period (-250–0 ms) of all accepted epochs. Spatial whitening was performed using the estimated noise covariance matrix. The SNR was assumed to be time dependent and automatically calculated as the power ratio of the whitened data. The time-dependent noise regularization parameter was set to the reciprocal of the SNR.

***2.3. Single-Subject Source Statistics.*** The eLORETA time series at each source point (Pascual-Marqui et al., 2011) consists of three waveforms corresponding to the amplitudes of the three dipole components in the x, y, and z directions. Hence we tested the null hypothesis at each voxel and time sample that the mean 3D current density vector was equal to the 3D zero vector using a multivariate Hotelling's $T^2$ test (Hotelling, 1931). The *p*-values corresponding to the $T^2$ values at each voxel and time point comprised the spatiotemporal *p*-maps that were inputted into group analyses.

***2.4. Subject Consistency Maps.*** For group analyses, the single subject $T^2$ and *p*-values obtained from the eLORETA estimates were aligned onto a common cortical atlas containing 14,584 voxels. To characterize the spatial consistency of *p*-values across subjects, group level subject consistency maps were constructed, showing at each voxel, the number of subjects surpassing a threshold at any time sample within the 400 ms post-touch window. In Experiment 1, the threshold was $p < 10^{-6}$ and the time window was 0-400 ms from the onset of the tactile stimulation. In Experiment 2, the threshold was $p < 0.001$ and the time window was the 400 ms after the rod touched the limb on the video (1100 ms). These maps (Figs. 3 and 5) provided intuitive summaries of the single subject statistics, because they were counts of numbers of subjects, but lacked a formal correction for multiple hypotheses, which motivated the subject partial conjunction test incorporating FDR control (*Section 2.5*).

***2.5. Spatiotemporal Subject Partial Conjunction (st-sPC) Group Analyses.*** Subject and cognitive conjunction analyses have received attention as alternatives to mixed/random effects analyses, because the latter can produce significant group results driven by a small number of subjects (Benjamini & Heller, 2008; Friston, Holmes, Price, Buchel, & Worsley, 1999; Heller, Golland, Malach, & Benjamini, 2007; Nichols, Brett, Anderson, Wager, & Poline, 2005; Price & Friston, 1997). For infant research, in particular, it is important to be able to take into account large inter-subject variability due to the differences in developing brains. Partial conjunction group analyses (Benjamini & Heller, 2008; Heller et al., 2007) allow reporting both group level significant effects and how many individual subjects show these effects (even in the case in which only a few subjects show a significant effect). These considerations motivated us to perform group analyses using spatiotemporal subject partial conjunction (st-sPC) mapping, which determines the minimum number of subjects with an effect, at each voxel and time point, under FDR control given multiple hypotheses. The method is equivalent to the spatial partial conjunction test developed for fMRI group statistics (Benjamini & Heller, 2008; Heller et al., 2007) but expanded to deal with the temporal aspect of the MEG source data.

As in all subject conjunction maps, our analyses evaluated the set-theoretic intersection (logical 'and') of subjects with significant activation. More specifically, we tested at every voxel and time point, whether at least *u* out of *n* subjects ($n = 14$) showed a real effect (i.e., significant under FDR control). Let $k(v, t)$ be the unknown number of subjects that show a real effect at a particular voxel and time point (i.e., the cardinality of the subset of subjects with a real response at that voxel and time point is $k(v, t)$). Then, the partial conjunction null and alternative hypotheses, at each voxel *v* and time point *t*, can be stated respectively as:

$$H_0^{u/n}(v, t): k(v, t) < u \text{ versus } H_1^{u/n}(v, t): k(v, t) \geq u$$

The conjunction null and the global conjunction null hypothesis are the special cases given respectively by $u = n$ (i.e., all subjects had an effect) and $u = 1$ (at least one subject had an effect). The *p*-values are independent across subjects, thus they were combined using Fisher's method (Fisher, 1925; Lazar, Luna, Sweeney, & Eddy, 2002). For testing the partial conjunction null hypothesis, $H^{u/n}(v, t)$, while correcting for multiple hypotheses, we combined the largest $n - u + 1$ *p*-values and performed FDR control (Benjamini & Hochberg, 1995; Genovese, Lazar, & Nichols, 2002) on the pooled *p*-value maps across all cortical voxels and time points within the 0–400 ms and 0–1750 ms time windows. Note that this procedure is repeated for all partial conjunction hypotheses of interest (in our case, $u = 1, 2, \ldots, n$). The *n* activation maps can be superimposed on the same image because the activation of at least *u* subjects is a subset of the activation map at *u'* subjects (for any $u' < u$).

***2.6 Source Event-Related Spectral Perturbation (ERSP) Analysis of Observed Touch.*** The spatially whitened sensor level signals were transformed to the time-frequency domain using complex Morlet wavelets (4–25 Hz in steps of 1 Hz and 20 ms) (Tallon-Baudry, Bertrand, Delpuech, & Pernier, 1996). The number of cycles of the wavelets were allowed to increase linearly from one to seven in the 4 to 25 Hz range in order to facilitate analysis of activity at lower frequencies. The lowest frequency (4 Hz) wavelet was 250 ms long, thereby constraining valid single trial wavelet coefficients to the -125–1615 ms time range. The wavelet transformed single trial data were then transformed to the source domain by multiplying them with the eLORETA inverse operator computed assuming an SNR of 1. The power at each source-point was then estimated by taking the square of the wavelet coefficient amplitudes and averaging them across the 12–18 Hz infant beta band. Power fluctuations were then expressed in dB units (i.e., ERSP) by taking the log of the ratio between the power and the pre-stimulus baseline power, and multiplying this by 10 (Makeig, 1993). These ERSP values were then interpolated to the cortical surface atlas for group analyses using spatiotemporal threshold-free cluster enhancement (TFCE). This consisted of first performing *t*-tests for each voxel and time point followed by the spatiotemporal TFCE transformation. Family-wise error rate correction for multiple hypotheses was carried out by thresholding the TFCE maps at a value corresponding to a corrected $p < 0.05$, based on the empirical permutation distribution of the maximum TFCE statistic obtained from each of the 10,000 Monte Carlo samplings of sign-flipped ERSP group data.

We focused on the infant beta band both because of previous adult studies implicating beta band oscillations in cognitive processes related to touch, and because the grand mean time-frequency power averaged across all voxels and all subjects indicated a clear increase in power in that frequency band. A power decrease in the infant alpha band (6-9 Hz) was observed, but it did not reach significance after FWER correction using TFCE.

## References


Benjamini, Y., & Heller, R. (2008). Screening for partial conjunction hypotheses. *Biometrics, 64,* 1215–1222.

Benjamini, Y., & Hochberg, Y. (1995). Controlling the false discovery rate—A practical and powerful approach to multiple testing. *Journal of the Royal Statistical Society, Series B, 57,* 289–300.

Fisher, R. A. (1925). *Statistical methods for research workers*. Edinburgh, Scotland: Oliver and Boyd.

Friston, K. J., Holmes, A. P., Price, C. J., Buchel, C., & Worsley, K. (1999). Multisubject fMRI studies and conjunction analyses. *NeuroImage, 10,* 385–396.

Genovese, C. R., Lazar, N. A., & Nichols, T. (2002). Thresholding of statistical maps in functional neuroimaging using the false discovery rate. *NeuroImage, 15,* 870–878.

Hämäläinen, M. S., & Sarvas, J. (1989). Realistic conductivity geometry model of the human head for interpretation of neuromagnetic data. *IEEE Transactions on Biomedical Engineering, 36,* 165–171.

Heller, R., Golland, Y., Malach, R., & Benjamini, Y. (2007). Conjunction group analysis: An alternative to mixed/random effect analysis. *NeuroImage, 37,* 1178–1185.

Hotelling, H. (1931). The generalization of student's ratio. *The Annals of Mathematical Statistics, 2,* 360–378.

Lazar, N. A., Luna, B., Sweeney, J. A., & Eddy, W. F. (2002). Combining brains: A survey of methods for statistical pooling of information. *NeuroImage, 16,* 538–550.

Makeig, S. (1993). Auditory event-related dynamics of the EEG spectrum and effects of exposure to tones. *Electroencephalography and Clinical Neurophysiology, 86,* 283–293.

Nevalainen, P., Lauronen, L., Sambeth, A., Wikström, H., Okada, Y., & Pihko, E. (2008). Somatosensory evoked magnetic fields from the primary and secondary somatosensory cortices in healthy newborns. *NeuroImage, 40,* 738–745.

Nevalainen, P., Pihko, E., Metsaranta, M., Sambeth, A., Wikstrom, H., Okada, Y., Autti, T., & Lauronen, L. (2012). Evoked magnetic fields from primary and secondary somatosensory cortices: A reliable tool for assessment of cortical processing in the neonatal period. *Clinical Neurophysiology, 123,* 2377–2383.

Nichols, T., Brett, M., Anderson, J., Wager, T., & Poline, J.-B. (2005). Valid conjunction inference with the minimum statistic. *NeuroImage, 25,* 653–660.

Pascual-Marqui, R. D. (2007). Discrete, 3D distributed, linear imaging methods of electric neuronal activity. Part 1: Exact, zero error localization. *arXiv:0710.3341*

Pascual-Marqui, R. D., Lehmann, D., Koukkou, M., Kochi, K., Anderer, P., Saletu, B., Tanaka, H., Hirata, K., John, E. R., Prichep, L., Biscay-Lirio, R., & Kinoshita, T. (2011). Assessing interactions in the brain with exact low-resolution electromagnetic tomography. *Philosophical Transactions of the Royal Society A: Mathematical, Physical & Engineering Sciences, 369,* 3768–3784.

Pihko, E., Nevalainen, P., Stephen, J., Okada, Y., & Lauronen, L. (2009). Maturation of somatosensory cortical processing from birth to adulthood revealed by magnetoencephalography. *Clinical Neurophysiology, 120,* 1552–1561.

Price, C. J., & Friston, K. J. (1997). Cognitive conjunction: A new approach to brain activation experiments. *NeuroImage, 5,* 261–270.

Tallon-Baudry, C., Bertrand, O., Delpuech, C., & Pernier, J. (1996). Stimulus specificity of phase-locked and non-phase-locked 40 Hz visual responses in human. *The Journal of Neuroscience, 16,* 4240–4249.

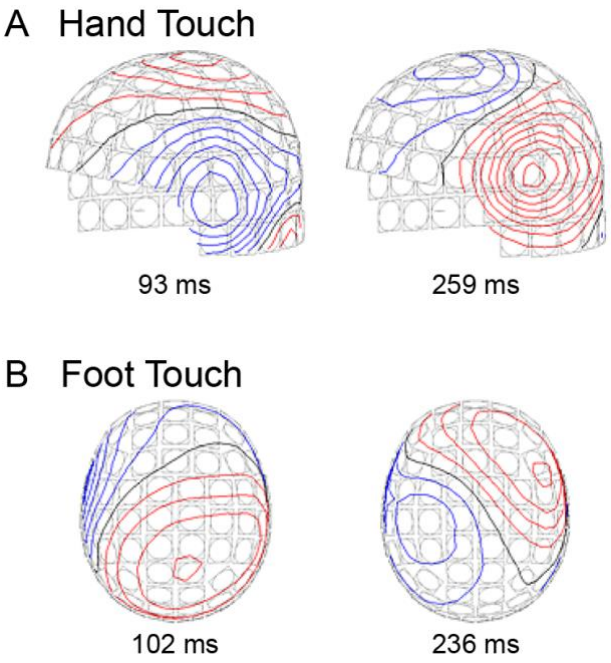


**Figure S1.** Experiment 1 grand-average magnetic field patterns at the four latencies shown in Table 1 (main paper) for tactile stimulation of (*A*) hand and (*B*) foot. The contour step is 5 fT.

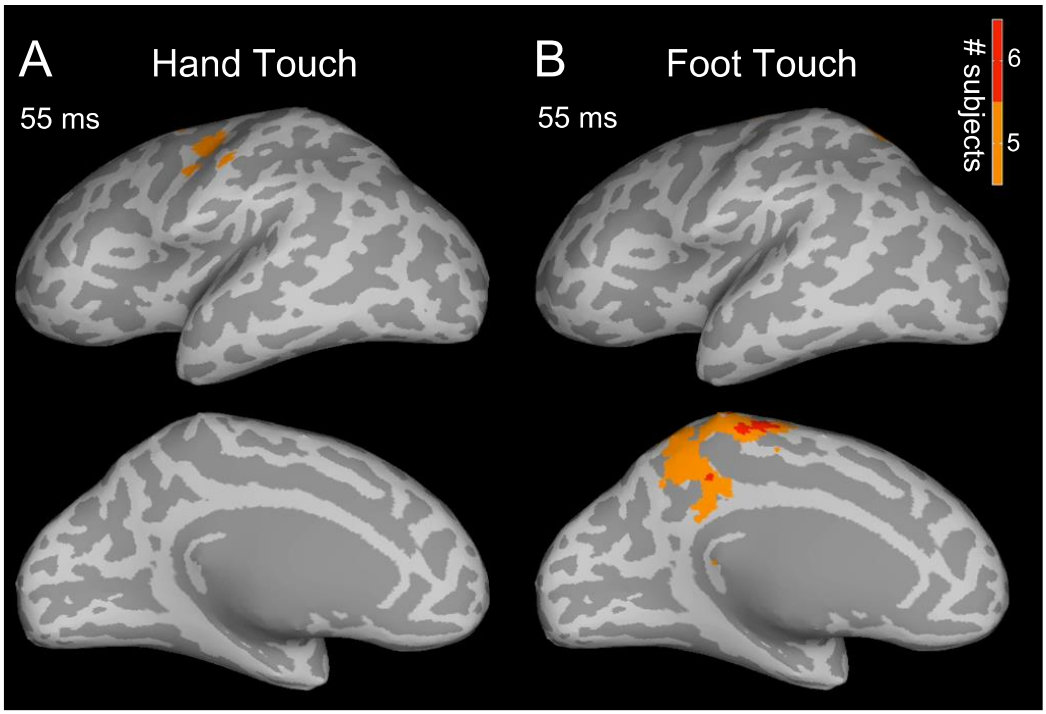


**Figure S2.** Experiment 1 spatiotemporal subject partial conjunction (st-sPC) maps showing early response to tactile stimulation (55 ms). Maps are visualized as in the main paper, displaying significant results for the two strongest hypotheses, $H_0^{5/14}$ and $H_0^{6/14}$ (i.e., at least 5 or 6 of the 14 subjects had a real effect, with FDR < 0.05) at 55 ms after the (*A*) hand or (*B*) foot touch onset. Stimulation resulted in activation in S1 (BA3, 1, 2) hand and foot regions respectively. A smaller number of significant subjects was obtained compared to the later latencies shown in Figure 4 (main paper). The data shown here may fit with reports of early responses to tactile stimulation of the tip of index finger in sleeping infants (Nevalainen et al., 2008; Nevalainen et al., 2012; Pihko, Nevalainen, Stephen, Okada, & Lauronen, 2009). We found that awake infants removed the tactile stimulator if it was attached to the index finger, thus we used the dorsal surface of the hand (and foot).

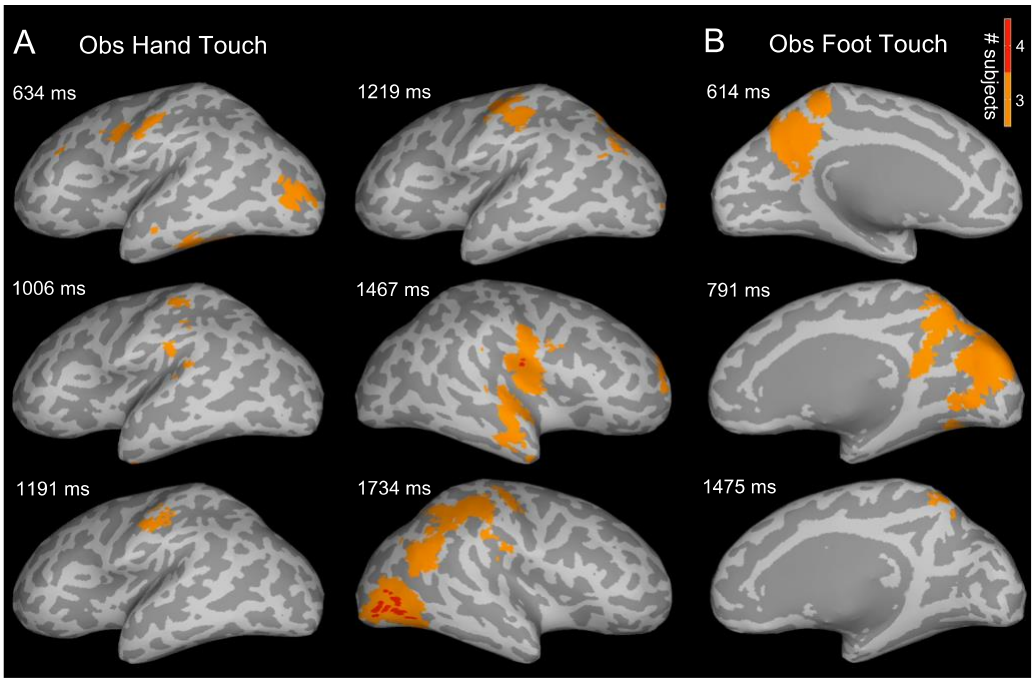


**Figure S3.** Experiment 2 spatiotemporal subject partial conjunction (st-sPC) maps at example latencies showing activation of somatosensory cortices (and other regions) in response to observed touch of (*A*) hand and (*B*) foot by a moving rod. Maps show the minimum number of subjects at particular voxels and time points with a significant effect with FDR < 0.05. Six examples are shown for hand and three for foot. *SI* Movies 3 and 4 provide dynamic visualizations of the st-sPC maps.

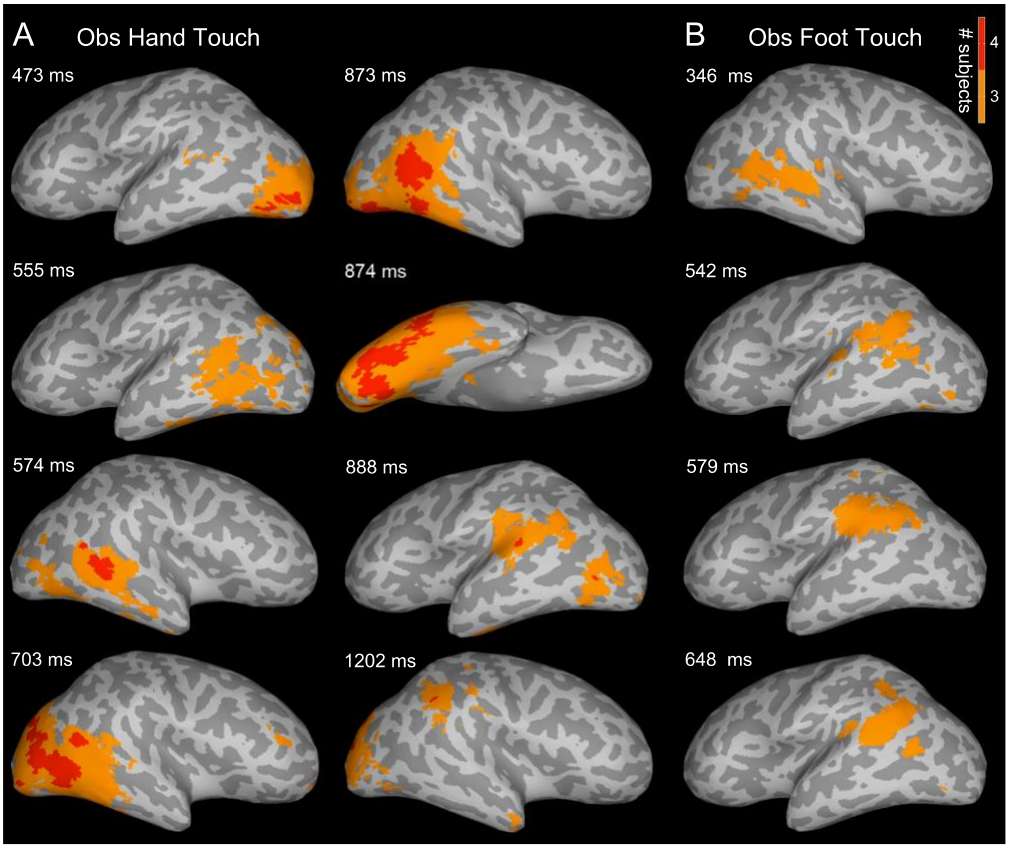


**Figure S4.** Experiment 2 spatiotemporal subject partial conjunction (st-sPC) maps at example latencies showing activation of regions thought to be involved in multisensory body, object, and self-other processing, in response to observed touch of (*A*) hand and (*B*) foot by a moving rod. Maps show the minimum number of subjects at particular voxels and time points with a significant effect with FDR < 0.05. Interestingly, significant activation was observed in regions associated with body processing such as, EBA, FBA, LOC, STS, and TPJ, as well as in other areas in parietal and frontal lobes. Eight examples are shown for hand and four for foot. *SI* Movies 3 and 4 provide dynamic visualizations of the st-sPC maps.

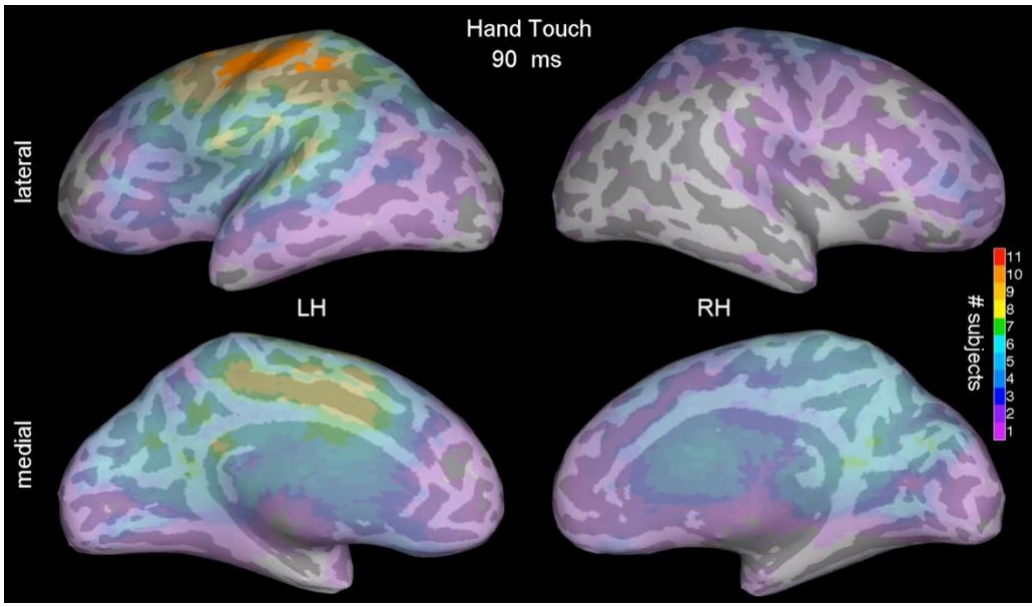


**Movie 1.** Experiment 1: Hand touch spatiotemporal subject partial conjunction (st-sPC) movie showing the minimum number of subjects (out of 14) with significant activation at each voxel and time point (ms). The rejected partial conjunction null hypotheses (FDR < 0.05) are visualized as colored nested areas from weakest (magenta) to strongest (red). The two strongest are shown using opaque colors; the rest are visualized using transparent colors. Example latencies from this movie are shown as static images in the main paper (Fig. 4A).

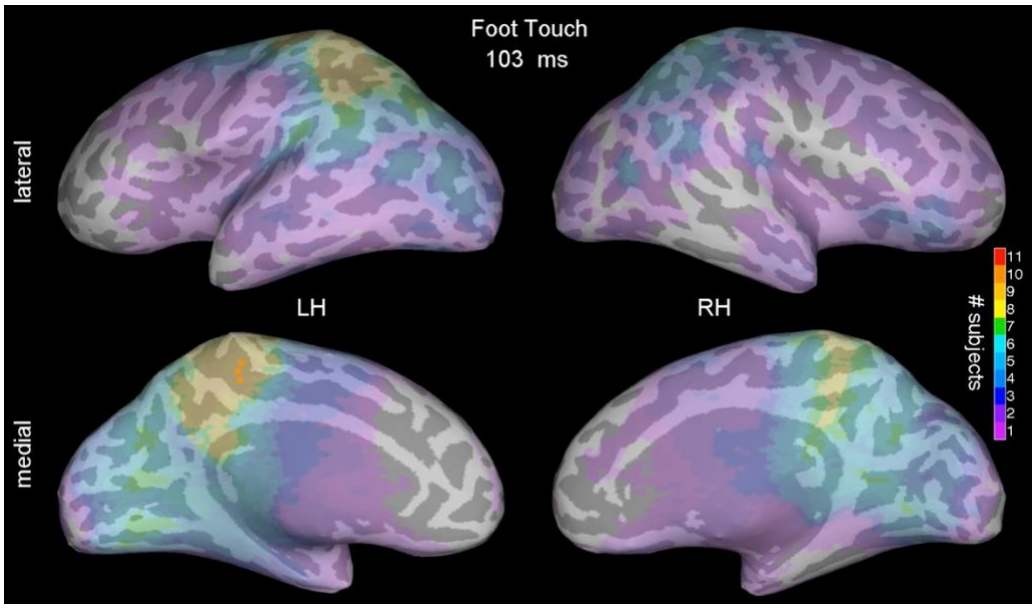


**Movie 2.** Experiment 1: Foot touch st-sPC movie. Visualization was done as in Movie 1. Example latencies are shown as static images in the main paper (Fig. 4B).

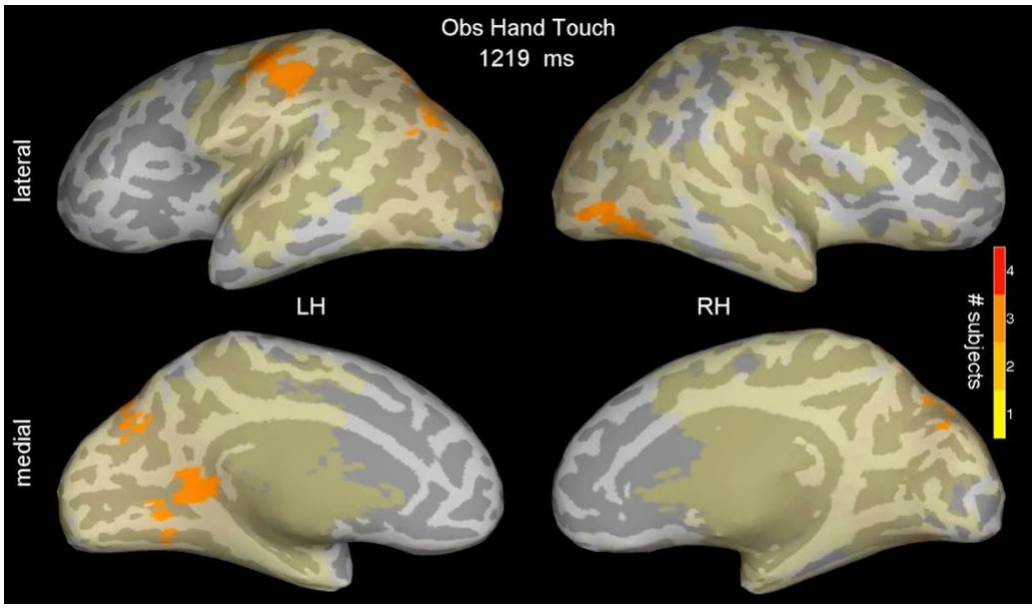


**Movie 3.** Experiment 2: Observed hand touch st-sPC movie showing the minimum number of subjects (out of 14) with significant activation at each voxel and time point. The rod-limb touch occurred at 1100 ms. The rejected partial conjunction null hypotheses (FDR < 0.05) are visualized as colored nested areas from weakest (yellow) to strongest (red). The two strongest are shown using opaque colors; the rest are visualized using transparent colors. Example latencies are shown as static images in *SI* Figs. S3 and S4.

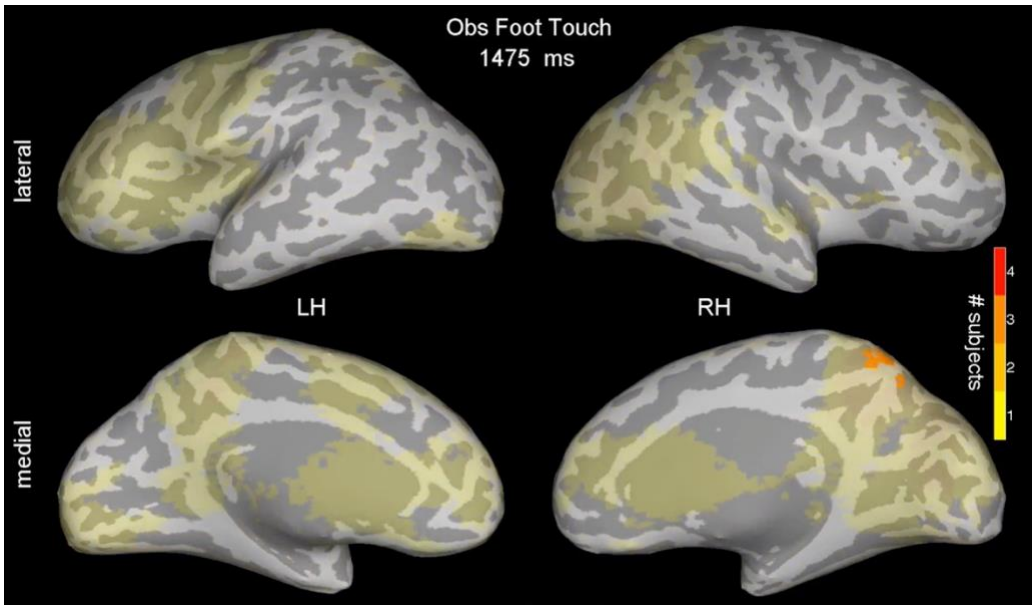


**Movie 4.** Experiment 2: Observed foot touch st-sPC movie. Visualization was done as in Movie 3. Example latencies are shown as static images in *SI* Figs. S3 and S4.

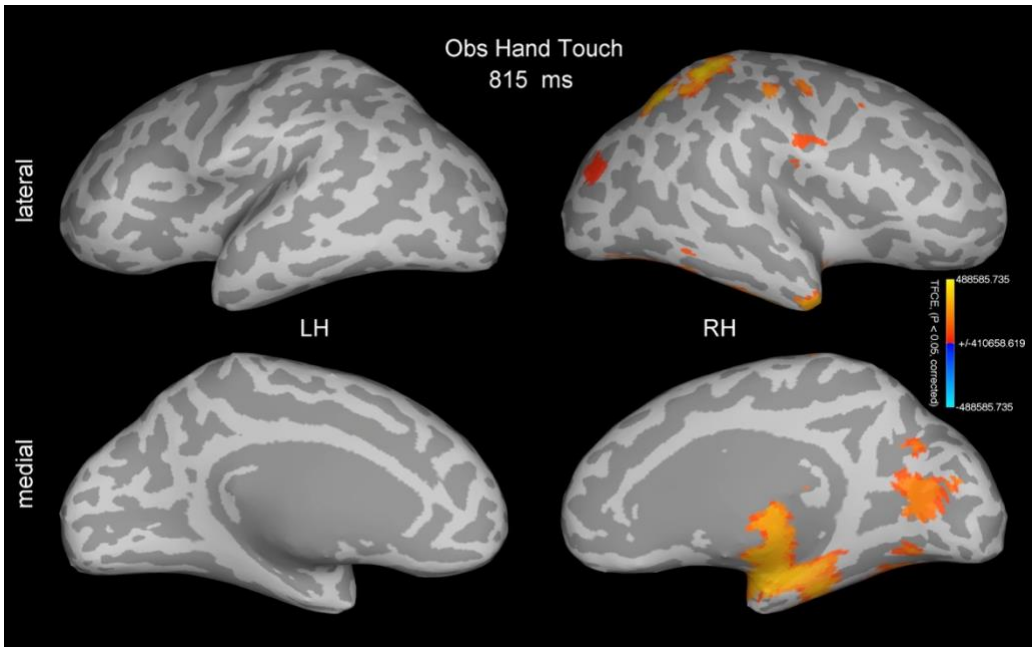


**Movie 5.** Experiment 2: Observed hand touch spatiotemporal threshold-free cluster enhancement (TFCE) statistical maps obtained for the infant beta band (12-18 Hz) event-related spectral perturbation (ERSP). TFCE values are thresholded at a value corresponding to $p < 0.05$ after family-wise error rate (FWER) correction for multiple hypotheses. Example latency is shown as a static image in the main paper (Fig. 6A).

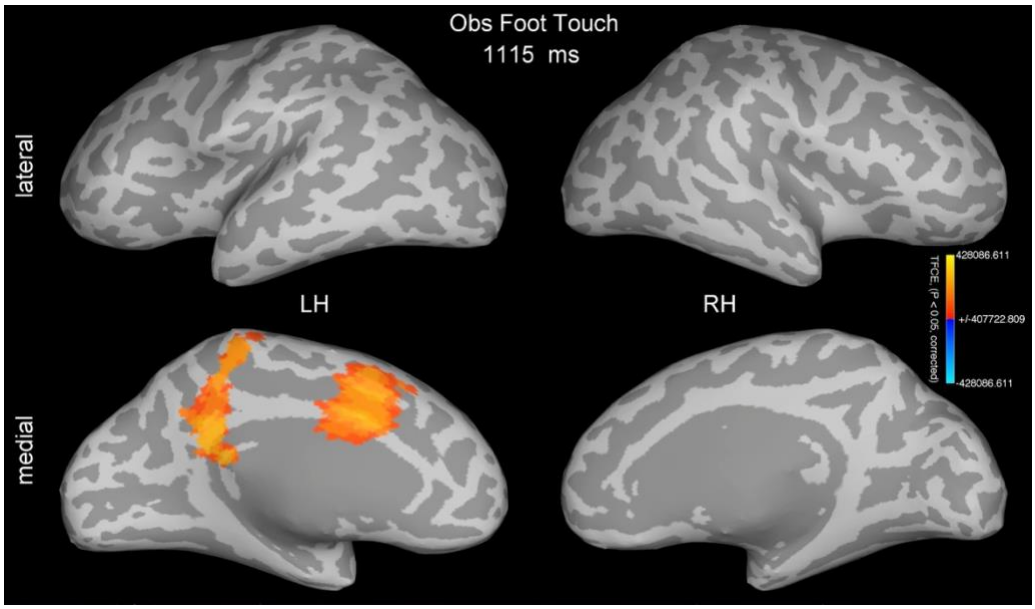


**Movie 6.** Experiment 2: Observed foot touch spatiotemporal TFCE statistical maps obtained for the infant beta band (12-18 Hz) ERSP. TFCE values are thresholded as in Movie 5. Example latency is shown as a static image in the main paper (Fig. 6B).